



PAPER • OPEN ACCESS

## Coating effects of a strain sensor on durability and sensitivity using the fiber loop ringdown spectroscopy technique

To cite this article: Burak Malik Kaya *et al* 2024 *Phys. Scr.* **99** 055511

View the [article online](#) for updates and enhancements.

You may also like

- [Sensory feedback by peripheral nerve stimulation improves task performance in individuals with upper limb loss using a myoelectric prosthesis](#)  
Matthew Schiefer, Daniel Tan, Steven M Sidek *et al.*
- [Fiber loop ringdown gas flow sensors](#)  
Haifa Alali and Chuji Wang
- [Realization of Elegant Security System for Women and Children Safety](#)  
Koteshwar Rao Danthamala, P Krishna, Y Srikanth *et al.*



## PAPER

## Coating effects of a strain sensor on durability and sensitivity using the fiber loop ringdown spectroscopy technique

## OPEN ACCESS

## RECEIVED

1 September 2023

## REVISED

21 February 2024

## ACCEPTED FOR PUBLICATION

25 March 2024

## PUBLISHED

4 April 2024

Original content from this work may be used under the terms of the [Creative Commons Attribution 4.0 licence](#).

Any further distribution of this work must maintain attribution to the author(s) and the title of the work, journal citation and DOI.



Burak Malik Kaya<sup>1</sup> , Okan Esenturk<sup>2</sup> , Celal Asici<sup>3</sup> , Umut Sarac<sup>4</sup> , Gokhan Dindis<sup>5</sup> and Mevlana Celalettin Baykul<sup>6</sup>

<sup>1</sup> Vocational School of Health Service, Eskisehir Osmangazi University, 26480, Eskisehir, Turkey

<sup>2</sup> Department of Chemistry, Middle East Technical University, 06800, Ankara, Turkey

<sup>3</sup> Department of Physics, Eskisehir Osmangazi University, 26480, Eskisehir, Turkey

<sup>4</sup> Department of Science Education, Bartin University, 74100 Bartin, Turkey

<sup>5</sup> Department of Electrical Electronics Engineering, Faculty of Sciences and Art, Eskisehir Osmangazi University, Eskisehir, Turkey

<sup>6</sup> Department of Metallurgical and Materials Engineering, Faculty of Sciences and Art, Eskisehir Osmangazi University, Eskisehir, Turkey

E-mail: [malikkaya@ogu.edu.tr](mailto:malikkaya@ogu.edu.tr)

**Keywords:** single-mode fiber, sensors, coated sensors, fiber optic sensors, fiber loop ringdown spectrometer, FLRDS, strain sensor

## Abstract

A sensor region in a single-mode optical fiber loop was created and utilized in order to study the coating effect on sensor durability and system sensitivity by the Fiber Loop Ringdown Spectroscopy (FLRDS) technique. The sensor system was simply designed without any additional optical components. The bending loss theory in the single-mode fiber (SMF) was taken into account in data calculation. After stretching was performed on 10.0 cm long coated and noncoated sensorheads from the mid-points, the strain detection limits were determined as 5.3345  $\mu\epsilon$  and 6.7497  $\mu\epsilon$  with bare and coated sensorheads, respectively. The purpose of this study is to analyze the effect of N,N-Diethyl-p-phenylenediamine (NDPD) coating of the sensorhead on the sensor durability and sensitivity. The baseline stability of the system was obtained as 1.18% by considering a hundred consecutive data. Regarding to obtained results, the difference between calculated total optical losses of FLRDS systems with noncoated and NDPD coated sensorheads shows that coating sensorhead enhanced the sensor durability and the system sensitivity. An FLRDS system with high sensitivity, simple design and easy setup offers real-time measurement with continuous monitoring and provides advantages on durability by modification the sensorhead such as NDPD coating. Due to its attractive features such as low cost, simplicity, easy setup, high sensitivity, increased durability and continuous monitoring, an FLRDS system has a wide range of application areas in structural health monitoring, transportation, early detection, biomedical, chemical trace elements, rail and asphalt applications for continuous monitoring in a real-time merit.

## 1. Introduction

Scientists have focused on fiber optic sensors (FOSs) for the last three decades because of their wide-range application area since FOSs provide high sensitivity, small size, low data loss, and long-distance applications. The Fiber Loop Ringdown Spectroscopy (FLRDS) technique, utilized with an FOSs system, is a multifunctional detection technique that evolved from the Cavity Ringdown Spectroscopy (CRDS) technique. Because two highly reflective mirrors are used as cavity region in the CRDS technique, an optical cable is used as the cavity in the FLRDS technique. The FLRDS technique is based on the time-domain because of the interaction of a small portion of laser pulse, which is confined into the loop with the measurands several times. Therefore, the FLRDS system measurement stability and sensitivity are excessively increased owing to the multiple interactions. The FLRDS technique has widespread application areas such as physical, chemical, and biological parameter measurement/monitoring and structural health monitoring [1–13]. Even if the other types of strain sensors are widely employed, the strain sensors of FOSs using the FLRDS technique are mostly utilized [14–20]. Among the

studied numerous parameters, two in fiber optical sensor systems, durability and sensitivity, are crucial to be improved due to enhancement of lifetime and detection limit [21–23]. For the investigation of the effect of NDPD coating on the durability and sensitivity of a sensor, a single-mode fiber (SMF) was chemically coated and tested by stretching from the mid-point after it was spliced to a fiber loop. The FLRDS technique utilized to analyze coating effect on durability and sensitivity offers several advantages, such as fast response with real-time monitoring and high sensitivity due to the multipass of a laser beam in the loop, resulting in multiple interactions with measurands,

Researchers are focused on strain detection using various fiber optic systems and different fiber types. Tarsa *et al* [24] used a 10 mm tapered fiber with a minimum displacement of 74 nm and a strain sensitivity of  $7.4 \mu\epsilon$ . This short sensor region and thinner tapered region have a negative impact on fragility and handling. Zhou *et al* [25] calculated the lowest strain value as  $3.6 \mu\epsilon$  by employing a 4.8 cm photonic crystal fiber (PCF) which is spliced into an SMF to create a Mach–Zehnder Interferometer (MZI) in a fiber loop with additional optical components such as an optical attenuator, Erbium Doped Optical Fiber Amplifier (EDFA), Fiber Bragg Grating (FBG), and optical spectrum analyzer (OSA). Their studies were carried out by using bare fiber, and their system and fiber types were different from those utilized in this study.

When a sensor region is covered/coated/encapsulated, another phenomenon comes into view. Because modifying sensorhead region may improve sensor sensitivity and durability, this improvement will improve not only the lifetime of the sensors in harsh environments, but also their sensitivity. Wang *et al* [21] studied the change in internal mechanism when the embedded insulation was adopted. They investigated in detail the mechanism of interfacial bonding in embedded optical fiber sensor by interfacial debonding between the host material and embedded sensors with the strain transfer theory. The same authors provide also a very good review on the strain transfer theory of fiber optics [26]. In several studies, the Surface Plasmon Resonance (SPR) technique was utilized to improve the sensitivity and durability of the sensors [27–33]. The purpose of enhancing the sensitivity and durability of the sensor is to enhance the key parameters of the system, e.g. the minimum detectable range or the system baseline, for the early detection in harsh environments such as underground for earthquakes or dams/buildings/bridges for micro cracks. Wang *et al* [34] studied also FBG and fiber optic sensor for monitoring 3D asphalt pavement deformation. They placed sensors in different layers on the  $y$ -axis and locations on the  $x$ -axes to analyze 3D displacement and strain change of asphalt pavement in heavy traffic and different temperature values.

In the current study, we analyzed the effect of NDPD coating on the sensorhead on the sensor durability and sensitivity. Easy setup and simple design FOS system was employed with the FLRDS technique so that it allowed fast response, high sensitivity, real-time monitoring, and portability. The target of this work is to study the enhancement of sensor durability and sensitivity by coating the sensorhead with NDPD. To analyze the results, the change in total optical losses of the system was compared when the strain was applied on a bare and NDPD coated sensorheads by pulling from the midpoints. The obtained results show that NDPD coating of the sensorhead affects the sensor durability, but do not crucially affects sensor sensitivity. With enhanced durability, this kind of sensor can be utilized in the structural health monitoring, land sliding, crack detection or wind turbine monitoring applications to take of advantage for longer lifetime and fast response with real-time monitoring.

## 2. Method

The laboratory setup of the FLRDS system is presented in figure 1. The system consists of an SMF coupled butterfly external cavity laser with 40 mW output power (Thorlabs, SFL1550S), its compact laser diode driver with thermoelectric cooler (TEC) and mount for butterfly packages (Thorlabs, CLD1015), a high speed and fiber-coupled InGaAs detector (Thorlabs, DET08CFC/M), 120 m SMF loop with  $2 \times 2$  identical 99.9:0.1 couplers (Opneti Communications Co. Shenzhen, China), a function generator, a 2 channel digital oscilloscope (Tektronix TBS1202B, Tektronix, Inc., Beaverton, OR, USA) and a basic FLRDS data collection and processing software. A noncoated sensorhead was created by removing protective plastic jacket from a part of fiber in the fiber loop and fixed on the holders as shown in figure 1. The stretching mechanism, shown in the inner figure on figure 1, was produced by a 3D printer to be able to move up to 15.0 mm by 0.1 mm steps and the stress was applied perpendicular to the sensorheads from the initial to the final positions. The noncoated sensorhead was stretched from the mid-point up to 9.0 mm by 1.0 mm steps. The NDPD (Sigma Aldrich,  $(C_2H_5)_2NC_6H_4NH_2$ ) coating was performed in following: The sensorhead was prepared in the same as noncoated sensor head. Afterwards, it was immersed into NDPD solution for 15 min. After it was left overnight on air for drying, the coated sensorhead was fixed on holders by using glue from two sides to eliminate sliding or loosening when the sensorhead was pulled. Figure 2 shows microscope images of the noncoated and coated sensorheads. The coated sensorhead was stretched from the mid-point up to 10.0 mm by 1.0 mm steps. Fiber sliding was diligently

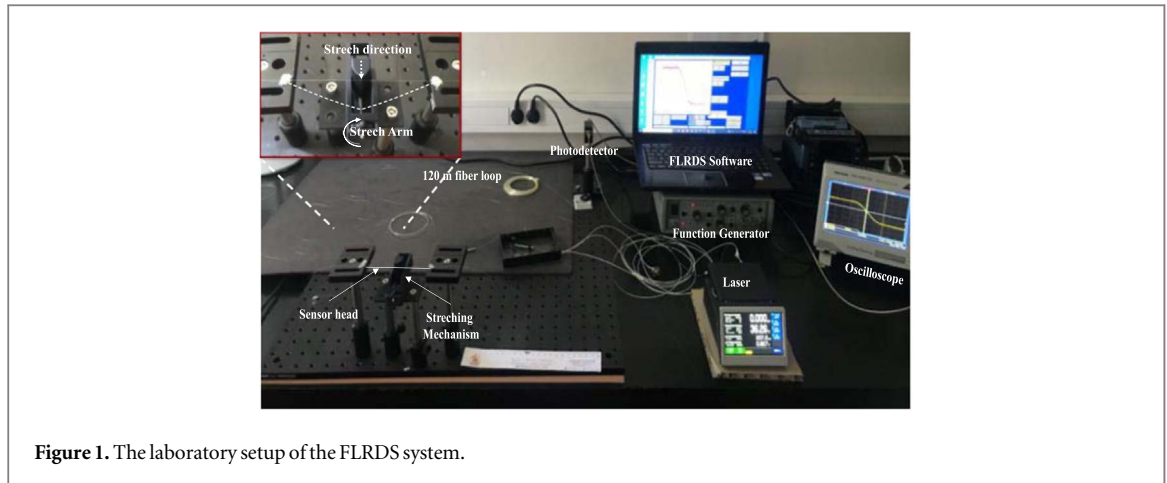


**Figure 1.** The laboratory setup of the FLRDS system.

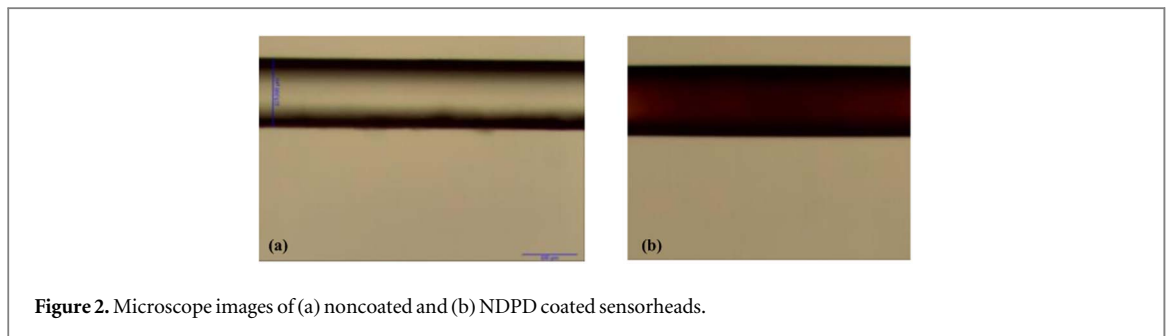


**Figure 2.** Microscope images of (a) noncoated and (b) NDPD coated sensorheads.

monitored during forced extension by marking the fiber. Any observable slide of fiber was recorded during the experiment when the coated and noncoated sensorheads were pulled from mid-points. The sensing mechanism was due to bending the optical fiber rather than the pure tensile mechanism. Therefore, the bending theory in SMF at 1550 nm is utilized to study sensitivity parameters of the FLRDS FOS system. As the 3D-printed puller stretched the sensorheads from the mid-points, an amount of bending loss was generated, resulting in a decrease in the RDTs. Stretching sensorheads from the mid-points increased the optical loss and caused a faster decay in RDTs.

The utilized bending theory in this study is well explained in the [35, 36]. The sensitivity calculation of the sensors because of strain and elongation of the fiber due to bending is defined in [37–39].  $\Delta L / L$  was utilized to calculate strain sensitivities ( $\varepsilon$ ), in which  $\Delta L$  is the length difference before and after extension and  $L$  is the original length of the sensorhead.

The working principle of the FLRDS sensor system is based on the monitoring decay of the laser beam within the fiber loop, rather than light intensity change. Therefore, the most distinguishing feature of the FLRDS technique is recording the decay time constant (referred to as ringdown time (RDT)) in a real-time manner. Two kinds of losses are considered in fiber optic transmission loss: i) intrinsic optical losses consist of absorption or scattering loss due to evanescent field dispersion on the sensorhead region, ii) extrinsic optical losses due to splicing, connector and bending.

The total fiber transmission loss includes the fiber absorption loss, the fiber couplers' insertion losses, and the fiber scattering loss is calculated by

$$A = \alpha L + E + \gamma \quad (1)$$

where  $\alpha$  is the wavelength-dependent absorption coefficient of the fiber core material (in  $\text{cm}^{-1}$ ),  $L$  is the fiber loop length,  $E$  is the total insertion loss of the fiber couplers, and  $\gamma$  is the total fiber scattering loss. In our study, splice loss as 0.01 dB, two identical connectors in the loop as  $0.17 \times 2 = 0.34$  dB and attenuation in 120 m fiber 0.03 dB are considered. Thus total loss per round 0.344 dB. Total transmission loss was calculated by using the Beert Lambert Law

$$\alpha_{dB} L = 10 \text{Log}_{10} \left( \frac{I}{I_0} \right) \quad (2)$$

which  $\alpha_{dB}$  light intensity attenuation per unit length in dB. From here, total transmission loss  $A$  and resulting theoretical RDT can be calculated.

A coupled light pulse into the fiber experiences several round trips in the fiber loop until it diminishes. Due to decreasing optical loss, the intensity of light pulse reduces after each round trip. Therefore, received signals by the photodetector have different intensities at every single round. Change in the intensity is written as [35]:

$$I = I_0 e^{-(Act/nL)} \quad (3)$$

where  $I_0$  is the intensity of the incident beam,  $A$  is the total transmission loss of the beam in fiber per round trip,  $c$  is the speed of light,  $n$  is the averaged refractive index and  $L$  is the total fiber loop length. The decreased time from  $I$  to  $I_0/e$  is called as ringdown time (RDT),  $\tau_0$ , and is given by equation (4):

$$\tau_0 = nL/cA \quad (4)$$

$$\tau = nL/[c(A + B)] \quad (5)$$

The total transmission loss remains constant for an FLRDS sensor since it is obtained by using the parameters of the fiber loop such as the fiber transmission loss, the absorption loss and the insertion losses in couplers. When a sensing action is created on the sensorhead such as applying a strain on it, an additional optical loss,  $B$ , is produced. The additional optical loss  $B$  is obtained by using equations (4) and (5) as:

$$B = (nL/c)(1/\tau - 1/\tau_0) \quad (6)$$

By using equation (6), whenever a sensing action is applied on the sensorhead such as pressure/strain or changing medium surrounding the sensorhead, the change in the total optical loss can be identified by using RDTs with and without the sensing action.  $B$  stands for created optical loss between two actions such as with no strain and applied strain on the sensorhead for this kind of FLRDS sensors. The amount of scattering loss in the evanescent field (EF) depends on the applied strain on sensorhead and hence monitored RDTs between stretches are different [1, 3, 11, 35]. The minimum detectable optical loss can be obtained by the following equation:

$$B_{\min} = (t_r/\tau_0)(\sigma/\tau_{ave}) = (1/m)(\sigma/\tau_{ave}) \quad (7)$$

where  $t_r$  is the time for a round trip of the laser beam inside the loop,  $m$  is the number of rounds, and  $\sigma$  is the standard deviation.  $\sigma/\tau_{ave}$  is the baseline stability.  $t_r$  and  $m$  are obtained as 489.4 ns and 31, respectively for 120 m loop. More details about the baseline stability and its calculation can be seen in [3, 11, 12, 35].

### 3. Results and discussions

#### 3.1. The system and fiber properties

Figure 1 shows the FLRDS system setup. Cladding and core diameters of a bare SMF are given by the producer (Corning, USA) as 125  $\mu\text{m}$  and 8.2  $\mu\text{m}$ , respectively. The system optical loss in total, including absorption loss, insertion loss and losses in the couplers when the laser pulse propagates into the fiber loop was found to be less than 0.40 dB due to the loss of fiber splice up to 0.01 dB.

A 14-pin butterfly external cavity laser diode was utilized to generate the laser pulse at a central wavelength of  $1550 \pm 0.5$  nm. It has 40 mW output power at the operating current and the operation temperature of 282 mA and 35.1  $^\circ\text{C}$ , respectively. The laser diode driver supplies the laser diode to control the working temperature and operating current. The function generator was square-modulated the generated laser pulse. While a small amount of the laser beam (0.1%) was coupled into the fiber loop by the first coupler, the rest of the beam was sent to the air by the coupler due to a 99.9:0.1 coupling ratio. Therefore, the separated beam can be utilized as a light source for another FLRDS system. As 0.1% laser beam propagates through the fiber loop experiencing several round trips, 0.1% of it is directed to the detector at the end of each round trip by the second coupler with the same coupling ratio (99.9:0.1). Hence, the photodetector collects the signals and sent to the oscilloscope to plot data.

Fiber optic cables are produced by using glass or plastic materials. The light is transmitted through the core of the fiber from one end to the other. The transmission process occurs in accordance with the total internal reflection (TIR) so that the core refractive index is higher than the cladding refractive index. Therefore, attenuation of the light obeys the Beer–Lambert Law. When fiber optic cables are compared to metallic conductors, the most advantageous feature of fiber optic cables is bandwidth, which is highly important for transferring more information to long distances with considerably low loss. Besides, fiber optic cables have many advantages such as electrical isolation and immunity to electromagnetic interferences, small size, flexibility, weight and portability [36, 39–41]. Fiber optic cables have widespread application areas from communication and illumination to power delivery and sensing.

A fiber optic cable comprises of core, cladding and plastic jacket as the protective layer. Depending on the guiding type of light in the core region, fibers can be classified into three groups: 1) multi-mode step-index fibers, 2) multi-mode graded-index fibers and 3) SMFs. In SMFs, since the light is guided through a path, only the fundamental mode (01 mode) is transmitted. The radius of fiber core and cladding in SMFs are given by the producer company (Corning, Inc. Co. NC, USA) as 8.2  $\mu\text{m}$  and  $125.0 \pm 0.7$   $\mu\text{m}$ , respectively [42]. The coating

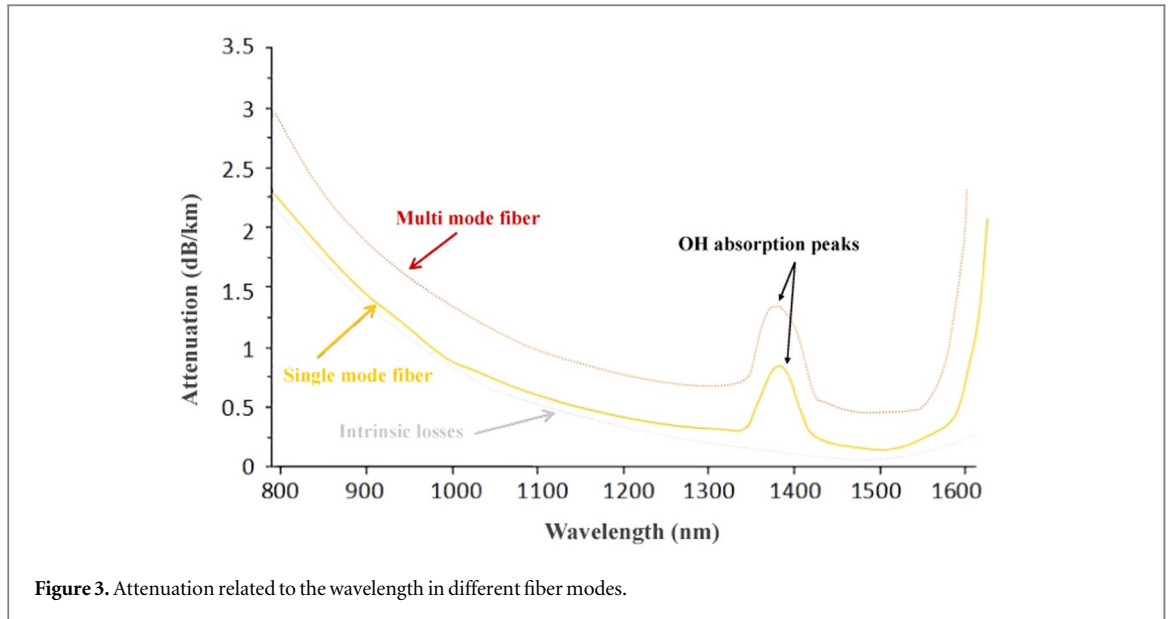


Figure 3. Attenuation related to the wavelength in different fiber modes.

diameter is given as  $242.0 \pm 5.0 \mu\text{m}$ . Since the light travels along a very narrow region, the reflection from the core-cladding interface is much lower than multi-mode fibers. An important parameter in SMFs is the numerical aperture (NA) value which is associated with the acceptance angle of the light into the fiber because the wavelength cutoff value, which is dependent on the NA, characterizes the fiber type. Below the cutoff wavelength value, higher-order modes can be transmitted with the zero-order mode. Therefore, wavelength cutoff value, hence NA value, plays a critical role in characterizing fiber characteristics whether it will be multi-mode fiber (MMF) or SMF.

Because the diameter of the core in an MMF is much bigger than an SMF, higher-order modes can be transmitted in multi-mode fibers. The core refractive index in multi-mode graded index fibers decreases radially outward to the core-cladding interface. Therefore, light propagates faster at the core-cladding interface than the core center. Even though multi-mode graded index fiber bandwidth is higher than step-index fibers, it is still lower than SMF bandwidths. MMFs having a wide range of core and cladding radii are available in the markets [43–46]. Generally, multi-mode graded index fibers are utilized for medium-ranged communications as local area networks.

In the current study, a bare SMF of 120 m at 1550 nm central wavelength was employed to setup the fiber loop. The selection reasons of SMF at 1550 nm central wavelength is following: (i) the long-distance transmission with a lower loss ratio, (ii) increasing sensitivity due to the interaction of narrower output laser pulse with measurands, (iii) as seen in figure 3, lower attenuation in this region.

The system optical loss is known as the attenuation, which is in decibels (dB) and calculated by:

$$A(\text{dB}) = 10 \log(P/P_0) \quad (8)$$

where  $P_0$  and  $P$  are the light power of input and output signals, respectively. The fiber attenuation is strongly dependent on the wavelength as shown in figure 3.

One of the parameters affecting the FLRD system sensitivity is the total optical loss which is related to the total attenuation. Several causes for attenuation in an optical fiber are known as the Rayleigh scattering, absorption and bending. For the Rayleigh scattering, refractive index variations in micro-scale of the core material will cause considerable light scattering, hence resulting in substantial optical loss. In our system, the Rayleigh scattering effect is very low due to its wavelength dependency. The absorption is slightly effective in the total loss of the system, but it is reduced significantly by the manufacturers by impurities. The bending is critical for the attenuation because the optical loss exponentially increases with decreasing bending radius [47]. Wang *et al* [21] studied interfacial debonding phenomena of embedded sensors based on strain transfer analysis, theoretical enhancement in interfacial bonding features and improvement in the durability of embedded sensors. The strain transfer mechanism is well-explained when strain perturbation occurs during embedment. They also analyzed the effect of radius and bonded length on the interfacial shear stress. Depending on the analysis, the shear stress increased with increasing bonded length. Her and Huang [48] validated a theoretical prediction and experimentally performed differential strains between the fiber optic strain sensor and test specimen by utilizing the Mach–Zehnder interferometric fiber optic sensor. Their results showed that strain in the test specimen was higher than measured in the laboratory medium. Ansari and Libo [49] studied the strain transferred from the host material to the surface-bonded optical fiber by proposing a theoretical model. They

assumed that coated fiber was perfectly bonded with host material when they neglected the effect of the adhesive layer.

### 3.2. Limitations, factors and optimization of the fiber optic sensor system with the fiber loop ringdown spectroscopy technique

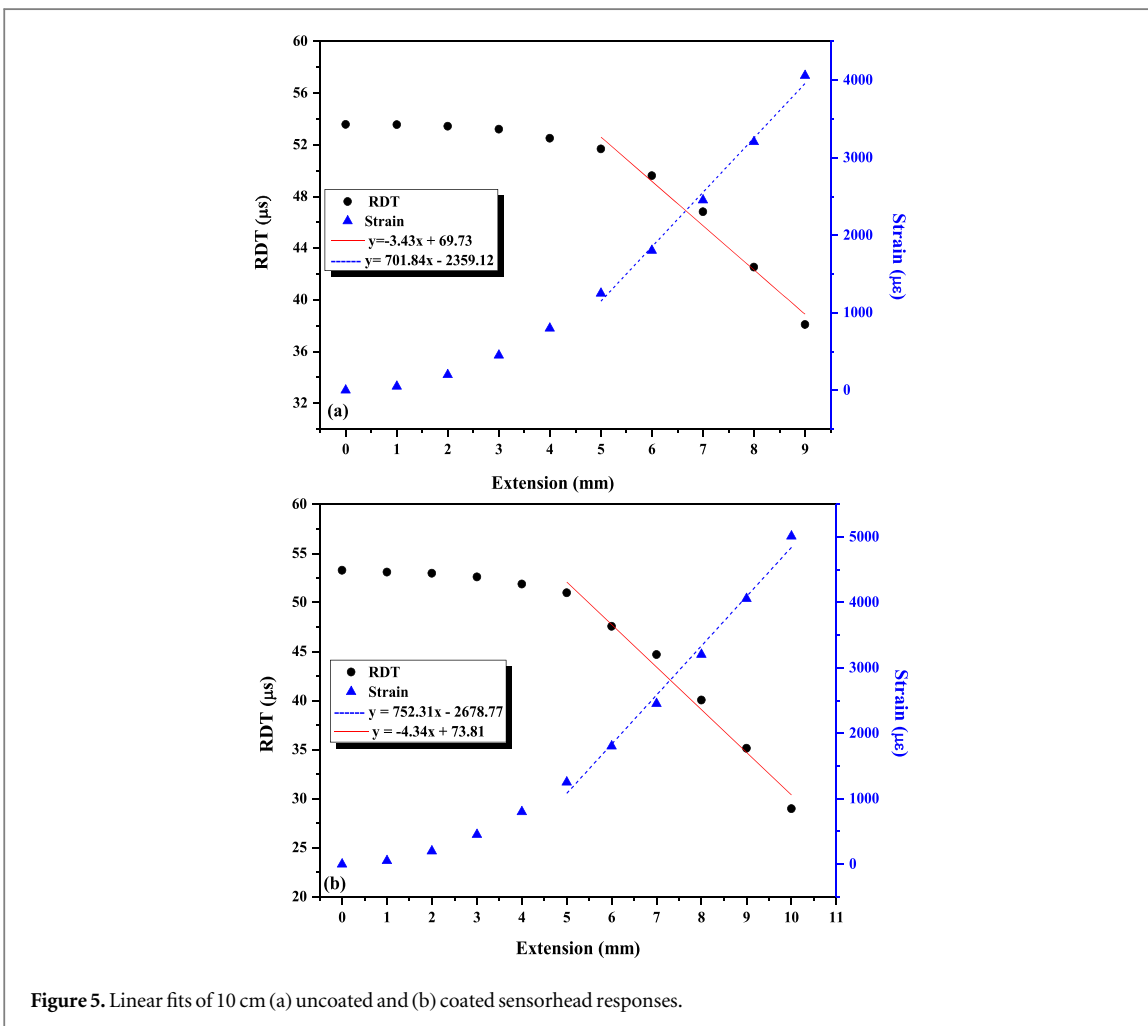
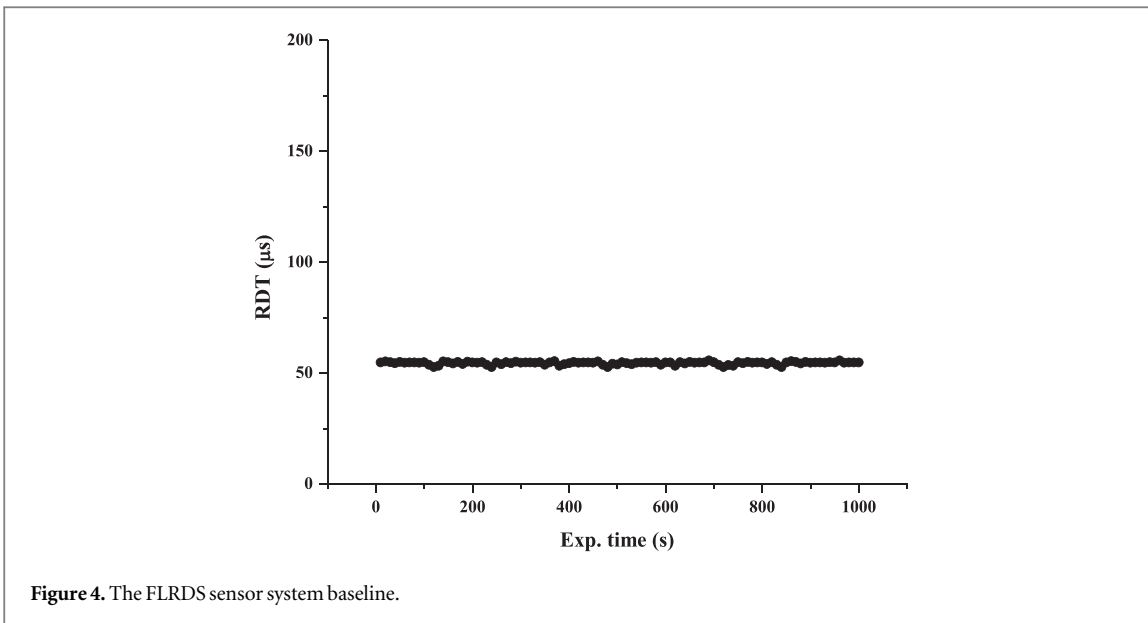
To setup a fiber loop ringdown system with a lower baseline stability and higher sensitivity, there are several factors to be optimized and combined with system components. First of all is the compatibility of system components such as the central wavelength of the laser source, fiber properties and the range of the photodetector. For example, if an appropriate fiber is not chosen related to the laser central wavelength, the system optical loss will be very high, resulting in the loss of outgoing signal. The second factor is the length of the fiber loop. In our study, a fiber loop designed by using 120 m SMF with  $2 \times 2$  two identical 99.9:0.1 couplers of 1.5 m arms were utilized. The total loss per round trip includes the insertion loss in two couplers, the fiber absorption loss, the splice loss and the attenuation loss was calculated as 0.3216 dB and A (percentage loss) was obtained as 7.14% by using equation (6). The total optical loss can be minimized by reducing the splice loss and choosing a shorter fiber loop length. The minimum fiber loop length can be estimated by features of the laser source. For example, if a laser source producing 5 ns pulses is utilized in a system, the minimum fiber loop length must be 1.02 m. Since a laser beam can travel 20.4 cm in the fiber core material ( $n_{\text{eff}} = 1.4682$ ) in 1 ns, the minimum required fiber loop length would be 1.02 m. Otherwise, two consecutive pulses will overlap before the first pulse is damped. If the fiber loop length is selected shorter (up to 1.02 m), we will get the lower laser beam attenuation. Because the most of total attenuation in the system comes from the couplers, changes in the total attenuation due to fiber length are reasonable. The third factor is a power source to minimize electrical fluctuations. Since a power source will supply stable electrical current, the baseline of the laser beam will be more stable. The fourth factor is the perfect adjustment of laser source parameters such as the laser current, the laser temperature, the laser driver temperature, etc. All parameters must be arranged diligently. The fifth factor is the fabrication of a sensitive sensorhead. The fabrication limits are extremely important since the optical loss of the system changes exponentially.

The FLRDS system was optimized by arranging the laser and its driver working parameters after the system setup. For the laser source, the given parameters in the user manual were not as good as achieving a higher sensitivity and a lower baseline stability. The optimum value for the laser current was scanned from 270 mA to 330 mA with 0.1 mA steps at 25 °C laser working temperature. After adjusting the best laser current value, the laser operating temperature value was scanned from 20 °C to 40 °C with 0.1 °C steps. The laser diode parameters were adjusted at 282 mA laser current and 35.1 °C laser operating temperature values. The minimum baseline stability was calculated depending on the aforementioned arrangement as 1.18% by using collected 128 averaged 100 data. Furthermore, laser driver parameters were setup and the FLRDS system was optimized. The original signal of the FRLDS system was adjusted to minimize signal to noise (S/N) ratio by arranging the aforementioned parameters. Minimizing the S/N ratio is extremely critical for an ultrahigh sensing system. The S/N ratio affects the system performance and signal quality so that it will process or transmit signals. The lower the S/N ratio, the lower the system can measure signals. To obtain the best RDT with the lowest S/N ratio, as in figure 4, laser driver current and temperature, laser diode current, function generator, and oscilloscope parameters were perfectly adjusted. For data collection, a special FLRDS software program was developed to accelerate, be reliable, and increase the collected data number. The software collected RDT data every 3 s and plotted it on a separate file automatically.

Figure 4 shows the baseline data of the FLRDS system with a noncoated sensorhead. 10 cm long sensorhead was fixed at the stages by the silicone and then the RDT of the sensor was recorded as 54.5  $\mu\text{s}$  with 0.643  $\mu\text{s}$  standard deviation. 100 data with 128 average was recorded with 10 s steps. Based on the data set, the baseline stability of the system was calculated as 1.18% by using  $1-\sigma$  standard deviation and the average RDT. The lowest detectable optical loss by this kind of system was obtained by using equation (7) as 105.96  $\mu\text{dB}$ .

Figure 5 shows both RDT and strain change related to extension for both the noncoated and the coated sensorheads. In figure 5(a), the noncoated sensorhead was stretched from the mid-point up to 9 mm with 1 mm steps. The RDT change between the first four data was very low, hence it can be attributed to the micro elongation of fiber and fixed points. Other data points showed a linear behavior with increasing stretch distance. Increasing extension causes a decrease in RDT, resulting in an increase in the optical loss, and an increase in stress. For the noncoated sensorhead, the strain sensitivity was calculated as 5.3345  $\mu\epsilon$ .

In figure 5(a), the optical loss between two adjacent data was calculated to show the FLRDS system sensitivity and the working principle. When the sensorhead was stretched 1 mm from the unstretched position, the change in the optical loss was calculated as 4.43  $\mu\text{dB}$ . This optical loss value is much lower than the system minimum detectable optical loss value. Hence, it cannot be measured by this kind of FLRDS system. Therefore, the optical loss change between the first four data values was attributed to the micro elongation of both fiber and on fixed



ends. The optical loss between the fourth and fifth data was calculated as  $125.1 \mu\text{dB}$ , which is higher than the measurable minimum optical loss and can be detectable by this kind of system. The noncoated sensorhead was stretched up to 9 mm because further stretching distances would cause the sensorhead to be broken.

For figure 5(b), the optical loss between two adjacent data can be calculated in the same way. The strain sensitivity was calculated as  $6.7497 \mu\epsilon$  for the coated sensor system. Since the FLRDS system sensitivity is the same, the system minimum measurable optical loss would be the same. Due to the optical loss change between



the first four data being lower than the detectable minimum optical loss by this kind of FLRDS system, it can be attributed to the micro elongations. The optical loss change between the fourth and fifth data is calculated as  $130.2 \mu\text{dB}$ , which is higher than this kind of FLRDS system minimum detectable loss. Therefore, this change can be measurable and the optical loss change between further stretched data can be observed. As shown in figure 5, it can be concluded that NDPD coating of the sensorhead increased the sensor durability, but did not critically affect the sensor sensitivity. The strains between the optical fiber as a sensor and the host structure are expected to be the same. Nevertheless, since a protective coating exists on the sensor, shear deformation is generated by the conversion of some part of the energy. Therefore, the strain of the bare fiber is different from that of the coated fiber.

In our previous study [35], 80 cm and 10 cm bare sensorheads were utilized with the FLRDS system of 0.22% baseline stability which was the lowest baseline stability in the literature by using bare SMF fiber with a fiber loop and placed between two discs. Sensorheads were stretched from the midpoints and the off-midpoints. 10 cm sensorhead was stretched 1 cm with 0.5 cm steps from the midpoint. The smaller the sensorhead length is, the smaller the extension distance is due to creating a higher optical loss, resulting in a broken sensorhead in the further extensions. In the current study, the behavior of the FLRDS system is similar to the FLRDS system in our previous work [35] when a 10.0 cm sensorhead was stretched from the midpoint. A couple of initial data is related to the sensorhead elongation and the rest presents a linear behavior. In another study, Habel and Bismarck [50] studied the polymeric coating effect of the synthetic optical fibers. They investigated the strength change of very thin organic layer-coated fiber in a concrete environment. They found that polymeric coatings survived the embedding procedure, the initial set and shrinkage during the hardening of concrete. Moreover, even though the polymeric coating increased the durability of fiber in the embedding process, the chemical processes in the cement mixture affected the sensor coating in the long-time. Wan *et al* [51] experimentally studied effects of adhesive parameters on strain transfer in the surface-attached of FBG sensor. They investigated strain transfer for surface attached fiber optic strain sensor by analyzing shear transfer effect through the adhesive and the polymeric coating on the fiber. Among the parameters of side width, top and bottom thicknesses, and the bond length, the bond length and the bottom thickness are the main factors affecting strain transfer.

As a result, in this work, 10 cm SMF from the fiber loop was used as sensorhead for both the noncoated and the NDPD coated, and stretched from the midpoints from the equilibrium positions to 9.0 mm and 10.0 mm with 1.0 mm steps, respectively. Results showed that the NDPD coated sensorhead performed better durability than the noncoated sensorhead. Therefore, sensors will be utilized in harsh environments or any other embedded systems can be coated to increase the sensor durability to be used in the long-term period. This kind of sensors with the FLRDS system may have attractive potential to be employed in embedded systems, structural health monitoring and physical, chemical or biological species detection applications with low cost, high sensitivity, fast response with real-time measurement and portability opportunity.

## 4. Conclusions

To investigate the effect of sensorhead manipulation in FOSs for durability and sensitivity enhancement purpose, a noncoated and an NDPD coated sensorheads of 10.0 cm lengths were stretched from the mid-points up to 9.0 mm and 10.0 mm with 1.0 mm steps, respectively. The lowest baseline, which plays an important role in calculating the minimum detectable optical loss of the FLRDS system, was calculated as 1.18% after system optimization. Depending on experimental results, the strain sensitivities of the noncoated and the NDPD coated sensors were calculated as  $5.3345 \mu\epsilon$  and  $6.7497 \mu\epsilon$ , respectively. The results presented that NDPD coating enhanced the sensor durability due to increasing strain sensitivity, but no observable effect in sensor sensitivity. Strain sensitivities of this kind of FLRDS sensors with no additional optical components such as OSA, FPI and FBG or any air-gap, have a high potential to be utilized for the early detection in various applications such as structural health monitoring, transportation, land sliding, wind turbine, railways, etc to determine strain in real-time.

## Acknowledgments

This research was supported by Eskisehir Osmangazi University (ESOGU) Scientific Research Project, Turkey, with the project code FHD-2021-1768 and partially supported by ESOGU Scientific Research Project, Turkey with the project code 201841074.

## Data availability statement

All data that support the findings of this study are included within the article (and any supplementary files).

## Conflict of interest

The authors declare that they have no conflict of interest.

## ORCID iDs

Burak Malik Kaya  <https://orcid.org/0000-0002-1251-6915>

Okan Esenturk  <https://orcid.org/0000-0001-6539-4344>

Celal Asici  <https://orcid.org/0000-0002-2628-0261>

Umut Sarac  <https://orcid.org/0000-0001-7657-173X>

Gokhan Dindis  <https://orcid.org/0000-0001-5642-7212>

Mevlana Celalettin Baykul  <https://orcid.org/0000-0003-2921-9762>

## References

- [1] Wang C and Scherrer S 2004 *Opt. Lett.* **29** 352
- [2] Hocker G B 1979 *Appl. Opt.* **18** 1445
- [3] Kaya M and Esenturk O 2020 *Turk. J. Elec. Eng. & Comp. Sci.* **28** 2789
- [4] Kaya M and Wang C 2017 *AIP Conf. Proc.* **1809** 020027
- [5] Yolalmaz A, Sadroud F H, Danişman M F and Esenturk O 2017 *Opt. Commun.* **396** 141
- [6] Kaya M 2020 *Turk. J. Elec. Eng. & Comp. Sci.* **28** 2375
- [7] Yolalmaz A, Danişman M F and Esenturk O 2019 *Appl. Phys. B* **125** 156
- [8] Wang C, Kaya M and Wang C 2012 *J. Biomed. Opt.* **17** 037004
- [9] Herath C, Wang C, Kaya M and Chevalier D 2011 *J. Biomed. Opt.* **16** 050501
- [10] Kaya M and Wang C 2014 *Fiber Optic Sensors and Applications XI* **9098** 90980O
- [11] Sahay P, Kaya M and Wang C 2013 *Sensors* **13** 39
- [12] Kaya M, Sahay P and Wang C 2013 *Sens. Actuators B: Chem.* **176** 803
- [13] Wang C, Kaya M, Sahay P, Alali H and Reese R 2013 *Optics and Photonics Journal* **3** 236
- [14] Qiu H, Qiu Y, Chen Z, Fu B and Li G 2008 *IEEE Sensors J* **8** 1180
- [15] Greenwood J and Dobre G 2000 *Proc. SPIE* **4075** 94
- [16] Seridevi S, Vasu K S, Asokan S and Sood A K 2016 *Opt. Lett.* **41** 2604
- [17] Lydon M, Taylor S E, Robinson D, Callender P, Doherty C, Grattan S K T and O'Brien E J 2014 *IEEE Sensors J* **14** 4284
- [18] Wang Y P, Xiao L, Wang D N and Jin W 2006 *Opt. Lett.* **31** 3414
- [19] Liu S et al 2015 *Sci. Rep.* **5** 7624
- [20] Li C, Zhang Y, Liu H, Wu S and Huang C 2004 *Sens. Actuators A: Phys.* **111** 236
- [21] Wang H, Jiang L and Xiang P 2018 *Opt. Fiber Technol.* **42** 97
- [22] Lu F, Wright R, Lu P, Cvetic P C and Ohodnicki P R 2021 *Sens. Actuators B: Chem.* **340** 129583
- [23] Bremer K, Alwis L S M, Zheng Y, Weigand F, Kuhne M, Helbig R and Roth B 2019 *Appl. Sci.* **9** 2476
- [24] Tarsa P B, Brzozowski D M, Rabinowitz P and Lehmann K K 2004 *Opt. Lett.* **29** 1339
- [25] Zhou W, Wong W C, Chan C C, Shao L Y and Dong X 2011 *Appl. Opt.* **50** 3087
- [26] Wang H, Xiang P and Jiang L 2019 *Sens. Actuators A: Phys.* **285** 414
- [27] Coelho L, Queirós R B, Santos J L, Martins M C L, Viegas D and Jorge P A S 2014 *In Proceedings of the Plasmonics in Biology and Medicine XI. International Society for Optics and Photonics* **8957** 89570K
- [28] Gu Z, Lan J and Gao K 2016 *Opt. Quantum Electron.* **48** 171
- [29] Hu H F, Deng Z Q, Zhao Y, Li J and Wang Q 2015 *IEEE Photon. Technol. Lett.* **27** 46
- [30] Wang W, Wu W, Huang J, Tian X and Fei X 2016 *In Proceedings of the Advanced Sensor Systems and Applications VII* **10025** 1–6
- [31] Lee Y K, Lee K S, Kim W M and Sohn Y S 2014 *PLoS One* **9** e98992
- [32] Frost S et al 2013 *Transl. Psychiatry* **3** e233
- [33] Nair R V, Yi P J, Padmanabhan P, Gulyas B and Murukeshan V M 2020 *Nanoscale Adv.* **2** 2693
- [34] Wang H, Xiang P and Jiang L 2018 *J. Lightwave Technol.* **36** 3624
- [35] Kaya M and Esenturk O 2020 *Opt. Fiber Technol.* **54** 102070
- [36] Fiber loop ring down spectroscopy for trace chemical detection 2013 *Thesis Work*
- [37] Ghimire M and Wang C 2017 *Meas. Sci. Technol.* **28** 105101
- [38] Ghimire M, Wang C, Dixon K and Serrato M 2018 *Measurement* **124** 224
- [39] Utilization of fiber loop ring down technique for sensing applications 2017 *Thesis Work*
- [40] Gupta M C and Ballato J 2006 *CRC Press* (Taylor & Francis Group)
- [41] Time-domain fiber loop ringdown sensor and sensor network 2013 *Thesis Work*
- [42] <https://corning.com/media/worldwide/coc/documents/Fiber/PI-1463-AEN.pdf>
- [43] Mitschke F 2009 *Fiber Optics* (Springer)
- [44] [https://thorlabs.com/navigation.cfm?guide\\_id=2284](https://thorlabs.com/navigation.cfm?guide_id=2284)
- [45] <https://edmundoptics.com/f/optical-grade-fiber-optics/11460/>
- [46] <https://guidingphotonics.com/hollow-fibers-optics-solutions-for-uv-and-visible-nir/#visible-nir>
- [47] Amanu A A 2016 *Adv. Appl. Sci.* **1** 1

- [48] Her S C and Huang C Y 2011 *Sensors* **11** 6926
- [49] Ansari F and Libo Y 1998 *J. Eng. Mech.* **124** 385
- [50] Habel W R and Bismarck A 2000 *J. Struct. Control* **7** 51
- [51] Wan K T, Leung C K Y and Olson N G 2008 *Smart Mater. Struct.* **17** 035037